Operation Mode Recognition of Surface Microdischarge Based on Digital Image Processing Techniques

Wenjiao Du
Guangdong Power Grid Company
Jiangmen Power Supply Bureau
Jiangmen, China

Chen Lu
Huazhong University of Science and Technology
State Key Laboratory of Advanced Electromagnetic Engineering and Technology
Wuhan, China

Zilan Xiong
Huazhong University of Science and Technology
State Key Laboratory of Advanced Electromagnetic Engineering and Technology
Wuhan, China
zilanxiong@hust.edu.cn

Zhenpeng Tang
Guangdong Power Grid Company
Jiangmen Power Supply Bureau
Jiangmen, China

Chongzhi Zhao
Guangdong Power Grid Company
Jiangmen Power Supply Bureau
Jiangmen, China

Xingyu Chen
Huazhong University of Science and Technology
State Key Laboratory of Advanced Electromagnetic Engineering and Technology
Wuhan, China

2021 IEEE 4th International Electrical and Energy Conference (CIEEC) | 978-1-7281-7149-4/21/$31.00 ©2021 IEEE | DOI: 10.1109/CIEEC50170.2021.9511033

***Abstract*—Surface microdischarge (SMD) has various application potential in biomedicine, agriculture and industry. An important issue for practical use is to develop an online monitoring method for operation mode recognition of SMD. In this paper, we proposed a operation mode recognition method for SMD based on digital image processing technique. The visible light digital images of SMD were shot and the RGB chromaticity index of the discharge images were extracted. It was found that the sum of all pixel values in the SMD discharge gray scale image and in the R, G, and B monochromatic images increased with the applied voltage monotonically, which can reflect the change of the discharge intensity. The difference between the proportions of the B component and the G component (Δ(B-G)%) showed a trend of first increasing and then decreasing as the applied voltage increased. The Δ(B-G)% reached the maximum value of 46.93% at V_{p-p} of 5kV and was corresponding to the mode transition point measured by Fourier transform infrared spectrometer (FTIR). Finally, a SMD operation mode recognition method, based on the Δ(B-G)% and the applied voltage was proposed.**

Keywords—surface microdischarge; operation mode; digital image processing; gray value; chrominance component

I. INTRODUCTION

In recent years, cold atmospheric plasmas (CAPs) has been widely applied in many fields, such as material modification, biomedicine, energy chemical industry, food processing and agriculture, *etc* [1-5]. A variety of CAPs sources have been reported to address requirements for these fields, including dielectric barrier discharge (DBD), plasma jet, corona discharge, gliding arc. Surface microdischarge (SMD) is a kind of DBD. Because of its simple discharge form, abundant active ingredients, and low processing temperature, SMD has been widely studied and applied. Lu *et al* adopted the SMD device to modify the mechanical properties of decellularized porcine aortic valve leaflets [6]. Xiong *et al* used the SMD device to treat model nails that had been coated on the backside of the nail with either bacteria or fungus, which showed a good sterilization result [7].

SMD has been reported to have different operation modes according to the dominating gas phase products, including ozone mode, transition mode and NO_x mode [8-9]. It is important to monitor the operation modes of SMD online in industrial applications. The current main methods for determining the operation mode of SMD usually directly detect the products under different conditions using spectrometer or NO_x sensors. These methods are valid, however, with disadvantages of high cost, complicated operation, and long time-consuming. Therefore, developing fast-responding, reliable and low cost diagnostic methods for the operation mode recognition of SMD has become a key issue in accelerating the industrial application of SMD.

With the development of digital image processing techniques, CAPs diagnostics based on these methods have been emerging recently, with the advantages of non-invasive , simple use, low price, and high real-time performance. Guo *et al* achieved the division of AC corona discharge stages and analyzed the spatial structure of AC corona discharge, though taking color images and using RGB and HSI chromaticity indicators [10]. Prasad *et al* used a color thresholding based image segmentation method to extract the effective spread of corona plasma, and analyzed the correlation between image parameters and corona power [11]. Wu *et al* identified the homogeneous and filamentary mode of DBD by analyzing the

This work was supported by Scientific Research Projects of China Southern Power Grid Corporation GDKJXM20184425 (030700KK52180140) and National Natural Science Foundation of China (51907076).

978-1-7281-7149-4/21/$31.00 ©2021 IEEE

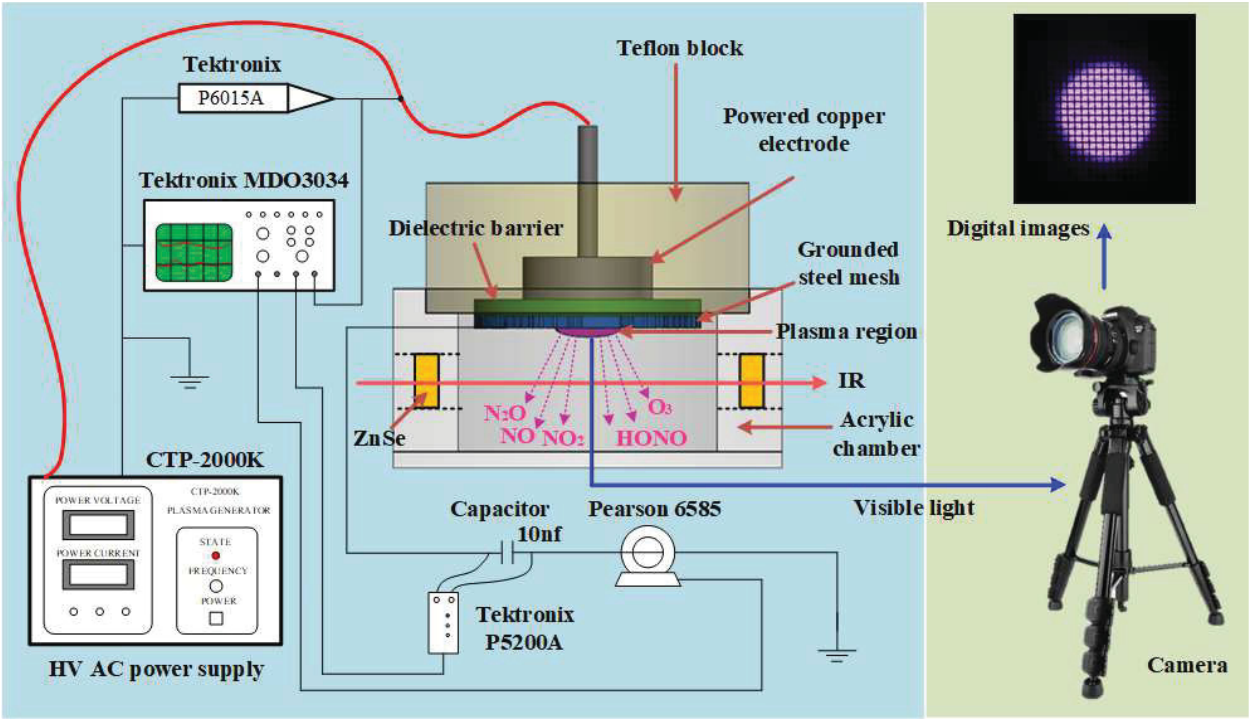

Fig. 1. The sketch of SMD and the expeiment setup

gray level histogram of the DBD discharge image, and verified the effectiveness of the method by changing the applied voltage, power frequency, and exposure time [12].

In this paper, we conducted preliminary study on using digital image processing techniques to detect the operation mode transition of SMD. FTIR was used to diagnose the gas phase products of SMD at different voltages to obtain the operation modes at different voltages. The digital camera was applied to catch the discharge images of the discharge in the corresponding operation modes under dark conditions. A SMD operation mode recognition method, based on combination of two features from the results, was proposed in this paper, by correlating the chromaticity information of SMD discharge images with its operation modes.

II. Experimenal Setup

A. Device Configuration

Fig. 1 shows the structure of the SMD device used in this paper. The power electrode made of copper was 20mm in diameter and 14mm in height, wrapped by Teflon. A wire mesh with a diameter of 50mm and a mesh density of 5×5 mesh/cm^2 was used as the ground electrode. A dielectric barrier made of Al_2O_3 (50mm in diameter and 0.5mm in thickness) was attached between the power electrode and the ground electrode. The SMD device was placed on top of a cylindrical acrylic chamber with a diameter of 38mm and a height of 45mm, which was used to store the gaseous chemical composition produced by the SMD device. Two ZnSe windows (13mm in diameter) were placed on the wall of the cylindrical acrylic chamber to transmit the IR beam for analyzing the composition of the gas phase products. A high-voltage and high-frequency AC power supply (Corona Lab, CTP-2000K) was used as the power source. For all the experiments, the waveform frequency was fixed at 8kHz. The applied AC voltage amplitude was monitored by a voltage probe (Tektronix P6015A) and an oscilloscope (Tektronix MDO3034) with a sampling gate up to 2.5GHz. A current probe (Pearson 6585) was used to measure the current of the circuit. A 10nF capacitor was connected in series between the woven wire mesh and the ground. The voltage across the capacitor was measured by a differential probe (Tektronix P5200A). Therefore, the power consumed by the SMD device can be obtained by the Lissajous method.

B. Gas-phase Spectroscopy

FTIR (Fourier transform infrared spectrometer, VERTEX 70, Bruker) was applied as an *in situ* diagnostic of the gaseous chemical composition produced by the SMD device. The wavenumber resolution of the FTIR measurements was set at 4cm^{-1}, and 16 scans were averaged to create each spectrum. The time resolution of each spectrum was 15s. The total measurement time of FTIR was consistent with the discharge time of the SMD device, both were 10 minutes. The primary gas phase products generated by the SMD device include N_2O, NO, NO_2, HONO, O_3. Fig. 2 shows a typical FTIR spectrum of the SMD device. It can be seen that, the main product of the SMD device at applied voltage V_{p-p} of 4kV is ozone, so we define the SMD device operates in ozone mode; when V_{p-p} increases to 9kV, the main products of the SMD are nitrogen oxides, so we simply define the operation mode as non-ozone mode in our study.

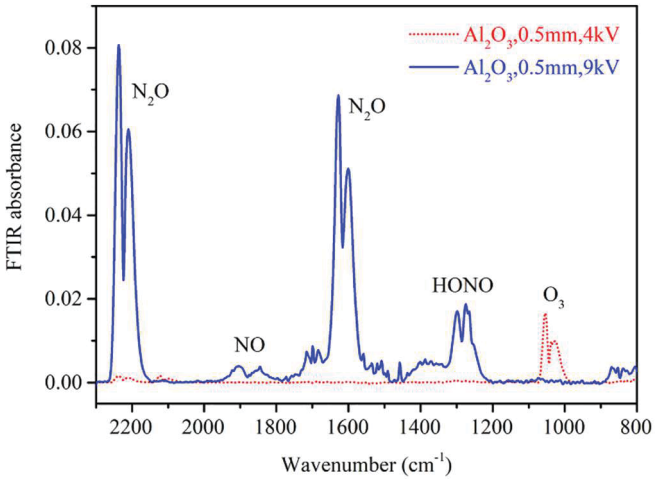

Fig. 2. Typical FTIR spectrum of the SMD device under different applied voltages.

C. Digital Image Processing Techniques for SMD

As shown in Fig. 1, the digital camera (NIKON D750) was used to obtain discharge images of the SMD under different voltages under dark background. The main camera parameters were set as follows: aperture f = 5.6, exposure time T = 1s, and ISO = 2000. The remaining parameters were set to default values. In order to avoid noise interference from the surrounding environment, the denoising and filtering measures on the captured discharge images were performed as follows: (a) Five SMD discharge images were taken continuously at the same voltage, while other conditions remain unchanged. (b) The image, when the applied voltage was 0kV, was used as the background image. And the SMD discharge images were compared with the background image to eliminate the interference of background noise. (c) For the same voltage, the final results were the average of five consecutive images.

The discharge color image was formed by superimposing three basic monochromatic images of R, G, and B. The SMD discharge gray scale image and the R, G, and B monochromatic images were analyzed in this study. First, for different voltages, the SMD discharge color image after denoising and filtering, was converted into the grayscale image. And the sum of all pixel values in the SMD grayscale image were extracted, as shown in formula (1). At the same time, the SMD discharge color image after denoising and filtering, was separated into three basic monochromatic images of R, G, and B. And the sum of all pixel values in the R, G, and B monochromatic images were extracted, as shown in formula (1). Then, the proportions of the R, G, and B components were calculated, as shown in formula (2).

$$S_i = \sum_{x=1}^{m}\sum_{y=1}^{n} f(x,y) \tag{1}$$

$$k = \frac{S_i}{S_R + S_G + S_B} \tag{2}$$

Here, S_i is the sum of all pixel values in the SMD discharge gray scale image or in the R, G, and B monochromatic images, m is the total number of pixels in the horizontal direction in the SMD discharge gray scale image or in the R, G, and B monochromatic images, n is the total number of pixels in the vertical direction in the SMD discharge gray scale image or in the R, G, and B monochromatic images, $f(x,y)$ is the each pixel value in the SMD discharge gray scale image or in the R, G, and B monochromatic images, k are the proportions of the R, G, and B components.

III. Results and Discussion

A. Division of the Operation Modes for SMD using FTIR

The operation modes of the SMD device at different applied voltages detected by FTIR method are presented in Fig. 3. When the value of the applied voltage $V_{p\text{-}p}$ is within 2.5kV to 5kV, the SMD operates in the ozone mode. When the value of the applied voltage $V_{p\text{-}p}$ is within 5.5kV to 10.5kV, the SMD operates in the non-ozone mode.

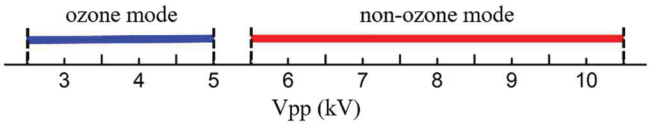

Fig. 3. Division of the operation modes for the SMD device by FTIR.

B. The Discharging Color Images vs. $V_{p\text{-}p}$

The discharge color images of the SMD device at different voltages were shot and shown in Fig. 4. Fig. 4(a) and (b) are the color images of SMD operating in ozone mode, Fig. 4(c) and Fig. 4(d) are the color images of SMD operating in non-ozone mode. It can be seen that, as the applied voltage $V_{p\text{-}p}$ increases, the discharge intensity of the SMD device becomes more severe, the discharge brightness of the SMD becomes stronger and the discharge area of the SMD becomes larger. At the same time, when the applied voltage $V_{p\text{-}p}$ is low, the place of discharge is mainly located at the interlace of the wire mesh. With the increase of the applied voltage $V_{p\text{-}p}$, the discharge area of each interlace of the wire mesh gradually expands and covers together, thereby forming a larger discharge area.

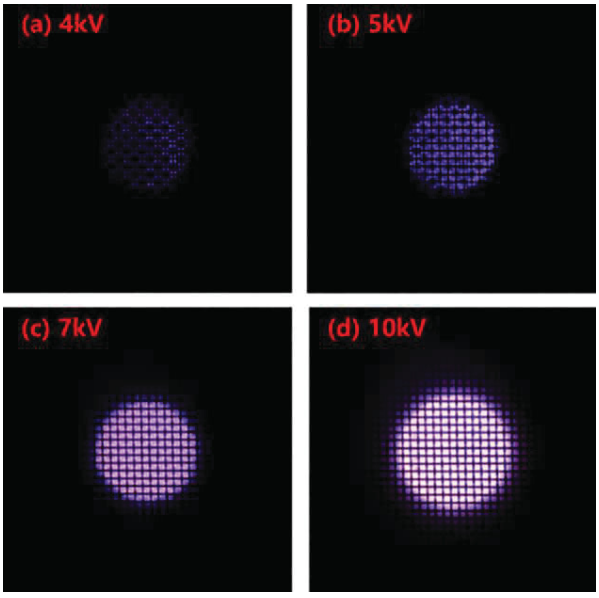

Fig. 4. The color images of discharge at different voltages

C. The Sum of All Pixel Values of the Discharging Area

In Fig. 5, the sum of all pixel values in the SMD discharge gray scale image and in the R, G, and B monochromatic images are shown as a function of the applied voltage $V_{p\text{-}p}$. It can be seen that, as the applied voltage $V_{p\text{-}p}$ increases, the sum of all pixel values in the SMD discharge gray scale image and in the R, G, and B monochromatic images increases monotonically. In addition, under the same applied voltage $V_{p\text{-}p}$, the sum of all pixels in the B component is the largest, followed by the sum of all pixels in the R component and the sum of all pixels in the G component. The sum of all pixel values could be used for $V_{p\text{-}p}$ or discharge power tracking in application.

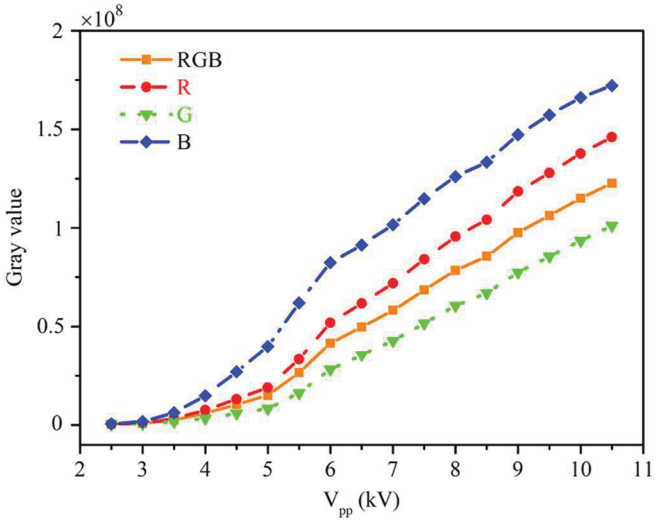

Fig. 5. The curve of the gray value with the applied voltage

D. The Relationship Between the Proportion of Chromaticity Components and the Operation Modes

In Fig. 6(a), the curve of the proportion of the R, G, and B components of the SMD device with the applied voltage $V_{p\text{-}p}$ is given. It can be seen that, when the SMD device operates in ozone mode, as the applied voltage $V_{p\text{-}p}$ increases, the B component gradually increases, the R component almost unchanged, and the G component gradually decreases. When the SMD device operates in non-ozone mode, as the discharge voltage $V_{p\text{-}p}$ increases, the B component gradually decreases, and the R component and G component gradually increases. For a same applied voltage $V_{p\text{-}p}$, the proportion of the B component is the largest, the proportion of the R component is the second, and the proportion of the G component is the lowest. When the applied voltage $V_{p\text{-}p}$ is 5kV, the proportion of B component reaches the maximum value, 59.31%. And the proportion value of G component reaches the minimum value, 12.37%.

In order to further analyse the relationship between the proportions of the R, G, and B components of the SMD device and the operation modes, as shown in Fig. 6(b), the curve of the difference between the proportions of B and G components with applied voltage $V_{p\text{-}p}$ is provided. When the applied voltage $V_{p\text{-}p}$ is within 2.5kV to 5kV in ozone mode, as the discharge voltage $V_{p\text{-}p}$ increases, the Δ (B-G)% sharply increases. When the applied voltage $V_{p\text{-}p}$ is 5kV, the Δ (B-G)% reaches the maximum value, 46.94%. When the applied voltage $V_{p\text{-}p}$ is higher than 5.5kV in non-ozone mode, as the discharge voltage $V_{p\text{-}p}$ increases, the Δ (B-G)% sharply decreases. This demarcation point is consistent with the mode transition point measured by FTIR (at 5kV).

From all the above results, it can be seen that the proportions of the R, G, and B chromaticity components of the SMD discharge images can reflect the useful information of the SMD in different operation modes. However, since the curve is parabola-like, we couldn't directly use the Δ (B-G)% value to recognize the operation modes of SMD. When in real application for an unknown SMD system, as the applied voltage is clear, it could be able to effectively identify the SMD operation modes through combining the feature of Δ (B-G)% and the applied voltage.

IV. Conclusion

In this paper, digital image processing technique was used to study the RGB chromaticity of SMD images. As the applied voltage increases, the discharge intensity, the discharge

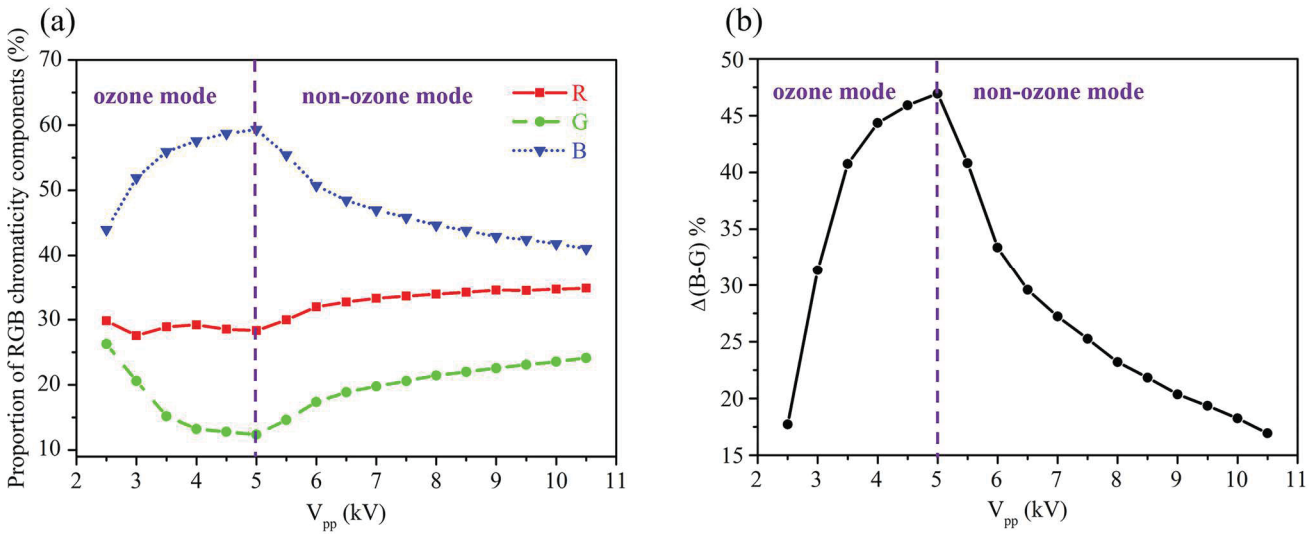

Fig. 6. The curve of proportion of chromaticity component with the applied voltage

brightness and the discharge area of the discharge images of SMD becomes larger. The sum of all pixel values could be used for V_{p-p} or discharge power tracking in application. The Δ(B-G)% curve can be used as an effective basis for online operation modes recognition of SMD. The highest point of Δ(B-G)% is corresponding to the operation mode transition voltage of SMD. Through combining the feature of the Δ(B-G)% and the applied voltage, the SMD operation modes can be effectively identified. The chromaticity index of the discharge images of SMD could be a potential method to offer online monitoring of operation modes. Future works, such as using other chromaticity systems, chromaticity indicators, and digital image processing techniques need to be conducted.

REFERENCES

[1] Z. Chen, R. Xu, P. Chen, and Q. Wang, "Potential agricultural and biomedical applications of cold atmospheric plasma-activated liquids with self-organized patterns formed at the interface," *IEEE Trans. Plasma Sci*., vol. 48, pp. 3455–3471, October 2020.

[2] X. Pei, D. Gidon, and D. B. Graves, "Specific energy cost for nitrogen fixation as NO x using DC glow discharge in air," *J. Phys. D: Appl. Phys*., vol. 53, pp. 1–6, November 2019.

[3] H. Zhang, J. Ma, J. Shen, Y. Lan, L. Ding, S. Qian, C. Chen, W. Xia, and P. K. Chu, "Comparison of the effects induced by plasma generated reactive species and H_2O_2 on lactate dehydrogenase (LDH) enzyme," *IEEE Trans. Plasma Sci*., vol. 46, pp. 2742–2752, August 2018.

[4] Y. Kusano, A. Bardenshtein and P. Morgen, "Fluoropolymer coated alanine films treated by atmospheric pressure plasmas − In comparison with gamma irradiation," *Plasma Processes Polym*., vol. 15, pp. 1–10, October 2017.

[5] Z. Xiong and D. B. Graves, "A novel cupping-assisted plasma treatment for skin disinfection," *J. Phys. D: Appl. Phys*., vol. 50, pp. 1–11, January 2017.

[6] C. LU, J. Dai, N. Dong, Y. Zhu, and Z. Xiong, "Investigation of air plasma generated by surface microdischarge for decellularized porcine aortic valve leaflets modification," *Plasma Processes Polym*., vol. 17, pp. 1–7, September 2020.

[7] Z. Xiong, J. Roe, T. C. Grammer, and D. B. Graves, "Plasma Treatment of Onychomycosis," *Plasma Processes Polym*., vol. 13, pp. 588–597, April 2016.

[8] M. J. Pavlovich, D. S. Clark, and D. B. Graves, "Quantification of air plasma chemistry for surface disinfection," *Plasma Sources Sci. Technol*., vol. 23, pp. 1–10, October 2014.

[9] T. Shimizu, Y. Sakiyama, D. B. Graves, J. L. Zimmermann, and G. E. Morfill, "The dynamics of ozone generation and mode transition in air surface micro-discharge plasma at atmospheric pressure," *New J. Phys*., vol. 14, pp. 1–11, October 2012.

[10] Z. Guo, Q. Ye, F. Li, and Y. Wang, "Study on Corona Discharge Spatial Structure and Stages Division Based on Visible Digital Image Colorimetry Information," *IEEE Trans. Dielectr. Electr. Insu*., vol. 26, pp. 1448–1455, October 2019.

[11] D. S. Prasad, and B. S. Reddy, "Digital Image Processing Techniques for Estimating Power Released from the Corona Discharges," *IEEE Trans. Dielectr. Electr. Insu*., vol. 24, pp. 75–82, February 2017.

[12] Y. Wu, Q. Ye, X. Li, and D. Tan, "Classification of Dielectric Barrier Discharges Using Digital Image Processing Technolog," *IEEE Trans. Plasma Sci*., vol. 40, pp. 1371–1379, May 2012.